International Journal of Applied Chemistry.
ISSN 0973-1792 Volume 13, Number 2 (2017) pp. 235-253

http://www.ripublication.com

Spectral, Kinetics of Thermal Decomposition and Computational Analysis of Bioactive Metal Complexes of 4 -Methoxysalicyldeoxime

Bibhesh K Singh[1], Jagdish Chandra[1], Hament K. Rajor[2] and Pinkee[1]

[1]Department of Chemistry, Govt. Postgraduate College, Ranikhet, Uttarakhand-263645, India.

[2]Department of Chemistry, Ramjas College, University of Delhi, Delhi-110007, India.

Abstract

Newly synthesized ligand 4-methoxysalicyldeoxime (4-MEOSDOX) and their Co(II), Ni(II), Cu (II) and Zn(II) complexes have been prepared and characterized by different physicochemical techniques. The ligand behaves as a bidentate ligand forming neutral metal chelates through the phenolic oxygen and the oxime nitrogen. The M–O stretching frequencies for the metal ions show good agreement with the Irving–William's stability order. Similar trend is seen for the M–N stretching frequencies in vibrational spectra and the shift in transitions from electronic spectral data for the metal complexes.Mass spectrum explains the successive degradation of the molecular species in solution and justifies ML_2 complexes. Electronic spectra and magnetic susceptibility measurements suggest square planer geometry of the metal complexes. The geometry of the complexes has been optimized with the help of molecular modeling. The bio-efficacy of free ligand and its metal complexes have been examined against the growth of bacteria *in vitro* to evaluate their anti-microbial potential.

Keywords: Bioactivity, Computational analysis, Metal complexes, Salicyldeoxime, Spectra, Thermal studies

1. INTRODUCTION

There is currently a renewed interest in the coordination chemistry of structurally modified bioactive oximes. Oximes play an important role in the development of transition metal coordination chemistry due to their versatile bonding mode. It may coordinate to one metal ion through the nitrogen atom and another metal ion through the oxygen atom. Oximes have both nitrogen and oxygen donor atoms; therefore, they link metals forming chelates. The hydrogen atom of the oxime =N–OH group can form potentially strong hydrogen bonds with other donor atoms or groups[1]. Thus, complexes bearing non deprotonated oximes may be considered as supramolecularsynthons, capable of forming extended supramolecular networks via hydrogen bonds. Oximes and their derivative are important intermediates in organic synthesis. They are also of interest as biologically active compounds. Many drugs have an oxime group in their structure, which is then frequently used for molecular modifications to develop new drugs and for synthesis of many functional groups as a starting point[1]. On the other hand, some of the oximes and their metal complexes exhibit liquid crystalline properties and having photo or electro-driven emitting properties[2].

Anti-tumour copper salicylaldoxime complex which induces Topoisomerase I (topo II) to form single-strand nicks in DNA and poisons its activity, which could be one of the possible mechanisms for the anti-cancer activity of this complex.Copper salicylaldoxime complex inhibits the enzyme activity through induction of enzyme linked single-strand breaks in the DNA and may inhibit topo II dimerization, which may lead to the formation of single-strand breaks[3].Topoisomerase II is a nuclear enzyme which iscrucial for resolving DNA knots in the chromosomes duringreplication, transcription and cell division duringchromosome segregation[3]. In acid medium, salicylaldoxime functions as a molecular ligand (H_2Sal), which brings about a decrease in electron density on donor atoms when compared with the HSal anion. Thus the ability of the used ligand to stabilize the central atom in unusually high oxidation states is impaired. The reaction of $Ni(HSal)_2$ with bromine involves a preferential attack on the aromatic ring of ligand. The possibility of oxidizing with peroxodisulfate is negatively affected by separation of nickel(II) salicylaldoximate from the water- organic solvent (ethanol, acetone) mixture[4]. However with increasing use of oxime as drugs and pesticides, the intake on these chemical followed by enzymatic oxidation may result in the formation of a variety of reactive intermediates, which may lead to cell and tissue damage [5]. Therefore, we report here in the synthesis, spectral characterization and kinetics of thermal decomposition of the complexes of 4-methoxysalicyldeoxime (4-MEOSDOX) ligand withCo(II), Ni(II), Cu(II) and Zn(II). The geometry of the complexes has been optimized through computational studies. The bioactivity of the ligand and its metalcomplexes possess antimicrobial potential.

2. EXPERIMENTAL

2.1 Material and methodology

All the chemicals used were of analytical grade and used as procured. Solvents used were of analytical grade and were purified by standard procedures. The stoichiometric analyses (C, H and N) of the complexes were performed using Elementarvario EL III (Germany) model. Metal contents were estimated on an AA-640-13 Shimadzu flame atomic absorption spectrophotometer in solution prepared by decomposing the respective complex in hot concentrated HNO_3. Their IR spectra were recorded on Perkin–Elmer FT- IR spectrophotometer in KBr and polyethylene pellets in the range 4000-400 cm^{-1} and 400-100cm^{-1}, respectively. ^{1}H-NMR spectra were recorded in DMSO-d_6 solvent (solvent peak 2.5ppm) on a Bruker Advance 400 instrument. Proton chemical shifts are reported in parts per million(ppm) relative to an internal standard of Me_4Si.The UV-Visible spectra were recorded in DMSO on Beckman DU-64 spectrophotometer with quartz cells of 1 cm path length from 200-900nm and mass spectra (TOF-MS) were recorded on Waters (USA) KC-455 model with ES^+ mode in DMSO. Magnetic susceptibility measurements were carried out at room temperature in powder form on a vibrating sample magnetometer PAR 155 with 5000G-field strength, using $Co[Hg(SCN)_4]$ as the calibrant (magnetic susceptibility $\approx 1.644 \times 10^{-5} cm^3 g^{-1}$).Rigaku model 8150 thermoanalyser (Thermaflex) was used for simultaneous recording of TG-DTA curves at a heating rate of $10^o min^{-1}$. For TG, the instrument was calibrated using calcium oxalate while for DTA, calibration was done using indium metal, both of which were supplied along with the instrument. A flat bed type aluminium crucible was used with α-alumina (99% pure) as the reference material for DTA. The number of decomposition steps was identified using TG. Computational analysis of the proposed structure of the complexes was performed using HyperChem professional version 7.51 program package[6].*In vitro* antibacterial activity of the synthesized compounds against *Streptococcus, Staph, Staphylococcus aureus* and *Escherchia coli* bacteria were carried out using Muller Hinton Agar media(Hi media) . The activity was carried out using paper disc method[7]. Base plates were prepared by pouring 10ml of autoclaved Muller Hinton agar into sterilized Petri dishes (9 mm diameter) are allowing them to settle. Molten autoclaved Muller Hinton had been kept at 48°C was incubated with a broth culture of the *Streptococcus, Staph, Staphylococcus aureus* and *Escherchia coli* bacteriaand then poured over the base plate. The discs were air dried and placed on the top of agar layer. The plates were incubated for 30 h and the inhibition zones (mm) were measured around each disc.

2.2 Synthesis of ligand and complexes

2.2.1 Synthesis of ligand

The ligand(Fig.1) has been synthesized by mixing 4-methoxysalicyldehyde (0.01M) with hydroxylamine hydrochloride(0.01M) in ethanol(25ml) at room temperature and addedtriethylaminedropwise with constant stirring by keeping the pH 8-9 for 48*h*.

The white precipitate was filtered, washed with ethanol and dried under vacuum over silica gel.

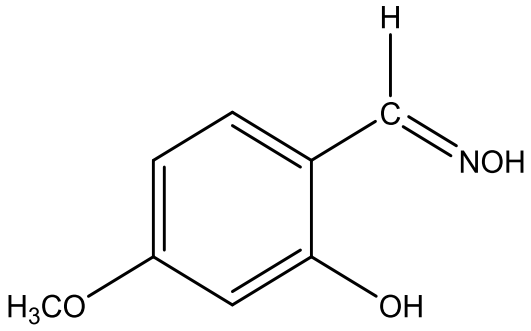

Figure 1: Structure of the Ligand(4-methoxysalicyldeoxime)

2.2.2 Synthesis of complexes

To 50 ml 0.2M aqueous solution of the salts of respective metal chlorides, 50ml. of 0.4M solution of ligand 4-methoxysalicyldehydeoxime(4-MEOSDOX) in 50% ethanol was added. The precipitated complexes were digested, filtered, washed with hot water and then with 20% ethanol and finally dried at 130 – 150 ^{0}C in an air oven. The Co(II) complex formed brown, Ni(II) complex formed Light green, Cu(II) complex formed Light blue and Zn(II) complex formed white precipitate. The solubility of these complexes is sparingly soluble in water and completely soluble in DMSO, Acetone etc.

3. RESULTS AND DISCUSSION

On the basis of elemental analysis data(Table1), the complexes have the general composition ML_2,where M=Co(II),Ni(II),Cu(II) and Zn(II);L=4-methoxysalicyldehydeoxime(4-MEOSDOX).The complexes were obtained in powder form. These were found to be soluble in Acetone and DMSO for spectral measurements. Various attempts to obtain the single crystals of the complexes have so far been unsuccessful.However, the analytical and spectroscopic data enables us to predict possible geometry of the complexes. The computational analysis helps to determine the bond angles, bond length and supports the possible geometry of the complexes.

3.1 Spectroscopic characterizations

The ^{1}H NMR spectra of a DMSO-d_6 solution of the oximeligand(MEOSDOX) show well resolved signals as expected. The spectrum of the oxime ligand shows a doublet at2.0 ppm (alcohol OH), singlet at 3.73ppm(-CH_3 group), singlet peak at 5.0ppm(aromatic C-OH) and multiplet peaks are at6.3ppm, 7.3ppm and 8.18ppm of benzylidenimin group.The ^{1}H -NMR spectra of complex II and complex IV show the resonance with expected integrated intensities. In both the complexes, no signal of the phenolic hydrogen indicates deprotonationof the ortho-hydroxyl group on complexation.

The IR spectrum of the free ligand showed a broad band between 3100- 3600 cm^{-1}, which can be attributed to phenolic OH group. This band disappears in all complexes, which can be supported the phenolic OH coordination. The metal phenolic group coordination in complexes is confirmed by the shift of *ν*(C-O) stretching band observed at1208 cm^{-1} in the free ligand to a lower frequency to the extent of 15–30 cm^{-1}[8]. The shift of *ν*(C-O) stretching band to a lower frequency suggests the weakening of *ν*(C- O) and formation of stronger M - O bond. The sharp and low intensity bands in the ligand due to *ν*(O-H) modes of N- OH groups in the 3100–2900 cm^{-1} frequency range shifted to the lower frequency region (2900–2800 cm^{-1}) which suggests the weakening of N-OH bond and formation of M-N bond[9] . The medium/strong bands observed in the 1610–1560 cm^{-1} frequency ranges in complexes were assigned to *ν*(C= N) mode, since the aromatic ring vibrations occurred in the same region, the C=N band was usually not clearly recognizable(figure 2a-e: IR spectrum of ligand and its complexes). The shift of *ν*(C= N) vibration to a lower frequency in the complexes suggests the nitrogen atom of the ring contributes to the complexation. The lower *ν*(C= N) frequency also indicates stronger M-N bonding[10,11]. The IR spectrum of the ligand showed the *ν*(N-O) band appears at 870 cm^{-1}. So, during complexation, *ν*(N-O) appeared at higher frequencies, indicating that N-O bond length decreases. The positive *ν*(N- O) shift indicates strengthening of the M- N bond. In the IR spectra of the complexes, a band is observed in the range 425-455 cm^{-1} that is attributed to the *ν*(M- N) stretching vibrations. The band appeared in the range 640-655 cm^{-1} due to the stretching vibrations *ν*(M-O) is assigned to the interaction of phenolic oxygen to the metal atom[8].

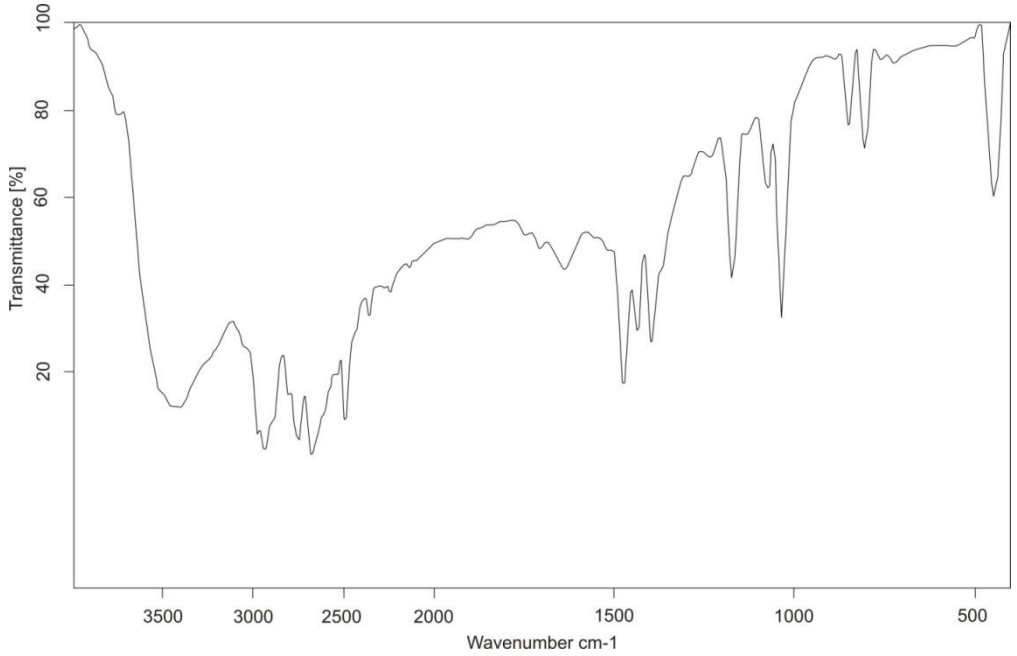

Fig.2 aIR spectrum of the ligand

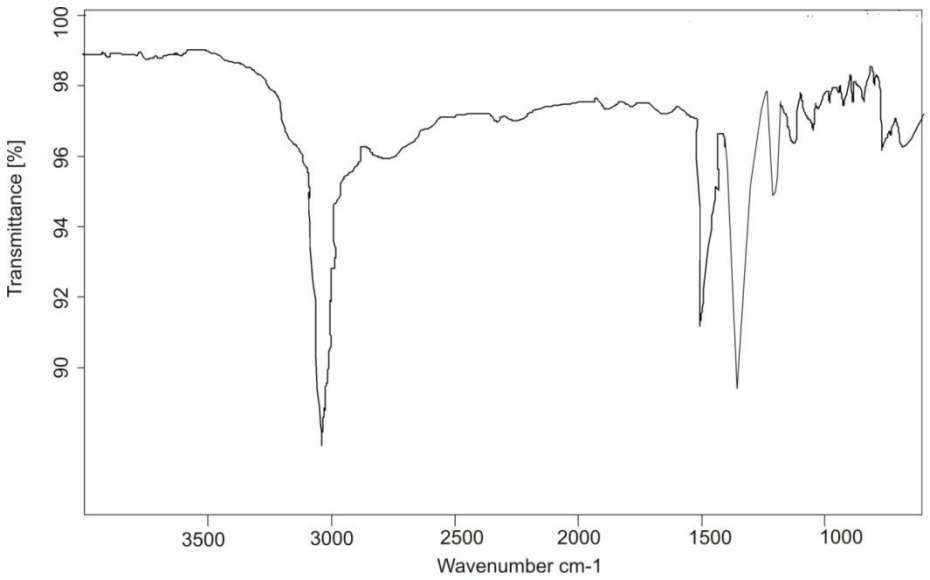

Fig.2 b.IR Spectra of the complex I

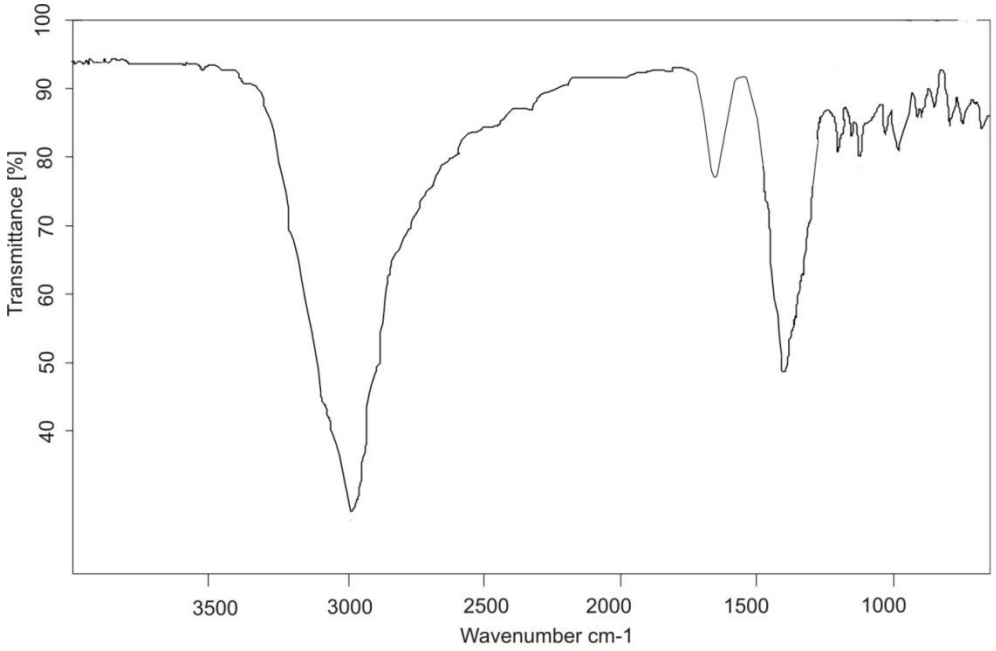

Fig.2c.IR Spectra of the complex II

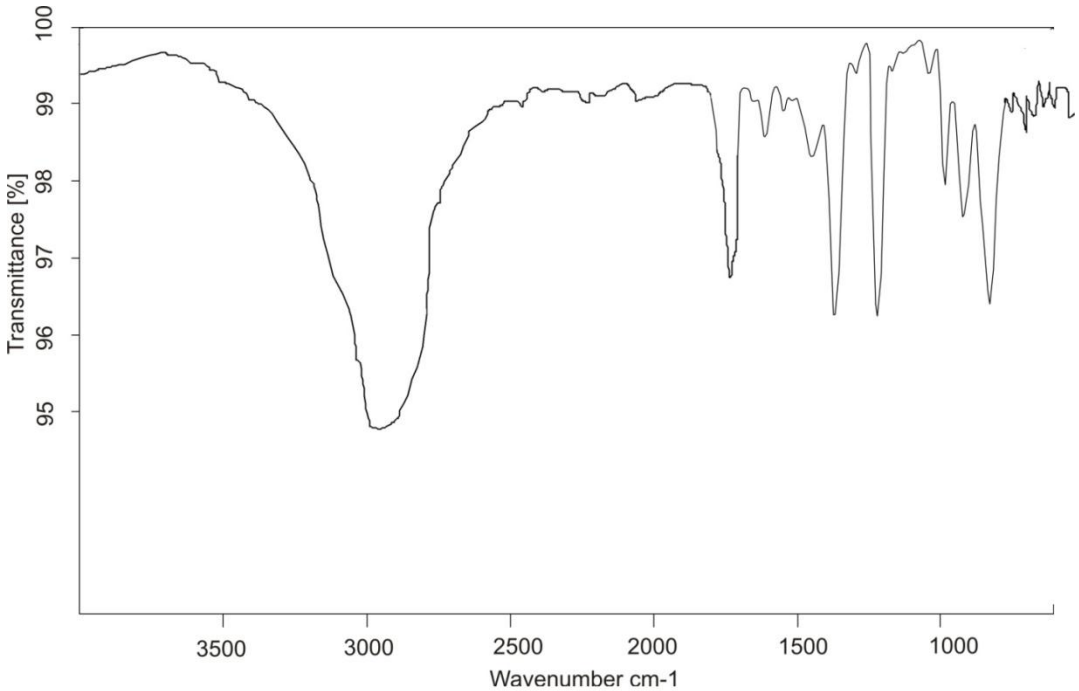

Fig.2 d.IR Spectra of the complex III

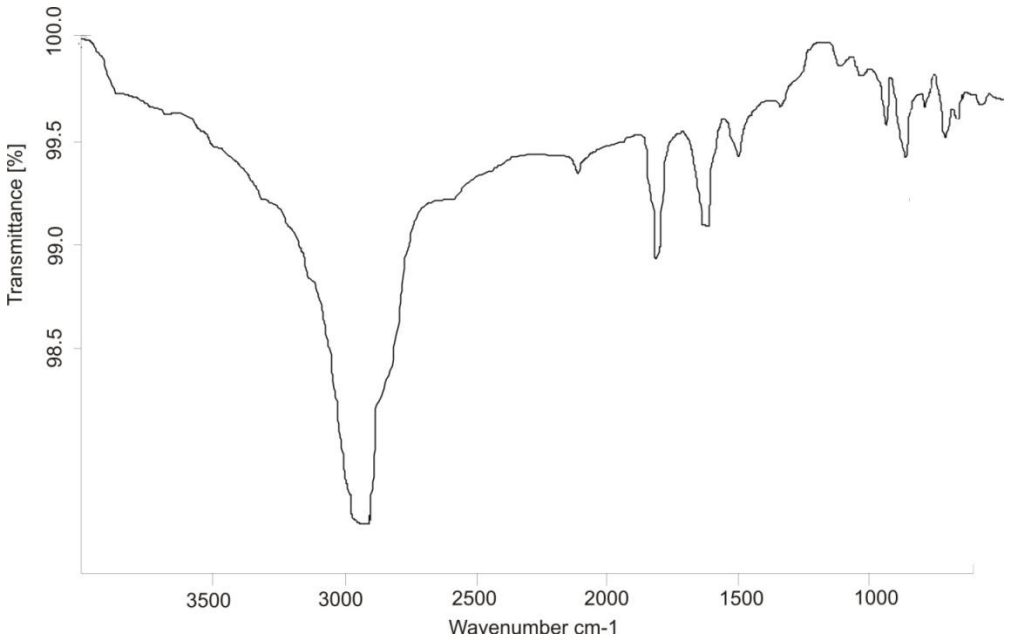

Fig.2e.IR Spectra of the complex IV

In the electronic spectra of the complexes, bands in the 220-375 nm regions coincide with the bands observed in the free ligand. Two relatively less intense bands (n →π* and π → π*) occur in the 220-375 nm region, these can be assigned to phenolic oxygen to metal and C=N to the metal charge transfer transitions, respectively. The electronic spectral data the Co(II) complexes show absorption bands at 525nm and 430 nm assignable to $^2B_{2g}\rightarrow{}^4E_g(P)$ and $^2B_{1g}\rightarrow{}^4A_{2g}$ (P) transitions, respectively, suggest square planar geometry of the complexes [12,13], which is also corroborated by magnetic moment value given in Table 1.

Table 1: Analytical and physical data of ligand and its complexes

S. No.	Compound/complex (Empirical formula)	Color	Decomposition temperature **(°C)**	Yield (%)	Analysis found (Calculated) (%)				μ_{eff}. (BM)	Electronic spectra (nm)
					C	H	N	M		
1	Ligand ($C_8H_9O_3N$)	White	143	86	57.48 (57.50)	5.38 (5.40)	8.38 (8.40)	-	-	220,375
2	Complex I $[Co(C_8H_9O_3N)_2]$	Brown	240	80	19.63 (19.66)	2.24 (2.28)	2.86 (12.10)	12.04 (12.06)	2.29	222,373,430,525
3	Complex II $[Ni(C_8H_9O_3N)_2]$	Light green	278	89	19.67 (19.70)	2.25 (2.30)	2.86 (12.00)	11.99 (12.02)	diamagnetic	223,376,545,648
4	Complex III $[Cu(C_8H_9O_3N)_2]$	blue	280	90	19.43 (19.45)	2.22 (2.26)	2.83 (2.88)	12.86 (12.90)	1.75	221, 379,522,660
5	Complex IV $[Zn(C_8H_9O_3N)_2]$	white	302	85	19.39 (19.41)	2.22 (2.33)	2.82 (2.99)	13.18 (13.20)	diamagnetic	225,378

The reason for the departure from the spin only value lies partly in the existence of the second order Zeeman effect between the ground and the higher ligand field terms

[14]. However, it lies mainly in the fact, that in the presence of spin-orbit coupling, the quenching effect of the ligand field cannot be complete. Spectra of the nickel(II) complex shows an absorption band at 648 nm, assignable to a $^1A_{1g} \rightarrow {}^1A_{2g}$ transition and band at 545nm assignable to a $^1A_{1g} \rightarrow {}^1B_{1g}$ transition which are consistent with square planar Ni(II) complex. It can be explained with the planar ligand set causes one of the d-orbitals ($dx^2–y^2$) to be uniquely high in energy and the eight electrons can occupy the other four d-orbitals but leave this strongly antibonding one vacant. The diamagnetic nature of the Ni(II) complexes further supports its square planar nature.The electronic spectrum of the Cu(II) complex shows very intense absorption bands in the UV region, attributed to ligand transitions($n \rightarrow \pi^*$ and $\pi \rightarrow \pi^*$), and a characteristic broad bands in visible region at 660 nm and 522 nm assignable to $^2B_{1g} \rightarrow {}^2E_g$ and $^2B_{1g} \rightarrow {}^2A_{1g}$ transitions respectively, indicates the possibility of square planar geometry of Cu(II) complex. The Cu(II) complex has magnetic moment value 1.75 BM reveals square planar geometry around the metal ion[12].Zinc(II) complex is diamagnetic in nature and their electronic absorption spectrum does not have d-d transition bands. These complexes assigned square planer geometry.

Mass spectrometry has been successfully used to investigate molecular species in solution [15]. The pattern of the mass spectrum gives an impression of the successive degradation of the target compound with the series of peaks corresponding to the various fragments. The intensity gives an idea of stability of fragments. The mass spectrum of the ligand having a molecular ion peak at 167{100% m/z} confirms purity of the ligand. The recorded molecular ion peaks of the metal complexes have been used to confirm the proposed formula. All the synthesized complexes containing metal ion were confirmed by good agreement between the observed and calculated molecular formula (Figure 3a-d: TOF-Mass spectrum of the complexes). Elemental analysis values are in close agreement with the values calculated from molecular formulas assigned to these complexes, which further supported by the TOF-mass studies. In the TOF–mass spectra of metal complexes initial fragmentation pattern is similar, a binuclear nature for these complexes $[M(L_2)]^+$ can be deduced. The mass spectrum of the complexes having a molecular ion peak at 390{46% m/z in complex I}, 391{45% m/z in complex II}, 395{46% m/z in complex III) and 397{38% in complex IV} respectively, further confirming the purity of the complexes. The prominent peak in the middle of the degradation pathway appears at positions (m/z values) 326(nearly 45% in complec I), 327(nearly 70% complex II), 331(nearly 40% complex III) and 333(nearly 48% complex IV) respectively are degradation of $[C_2H_8O_2]^+$ molecule and the result of demetallation and subsequently a partial intramolecular hydrogen bonding. Likewise peaks around 223-231(m/z) and 167(m/z) are attributable to unstable monomeric species as $[M(L)]^+$ and $[H_2L]^+$ respectively, usually present in the mass spectra of these systems [16].

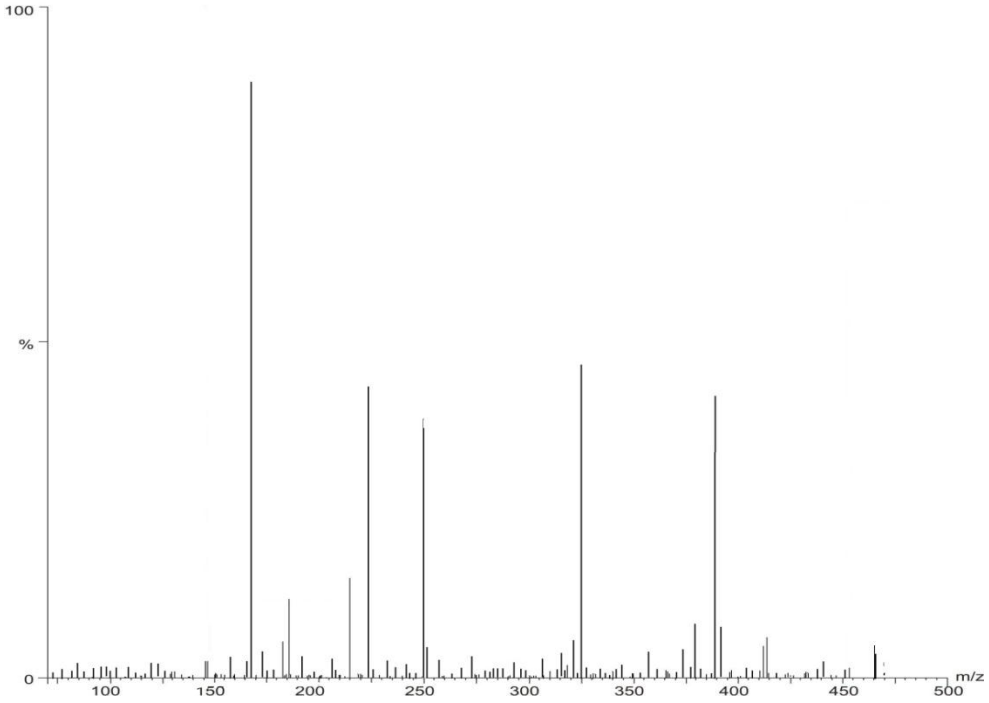

Fig.3 a. TOF mass spectrum of the complex I

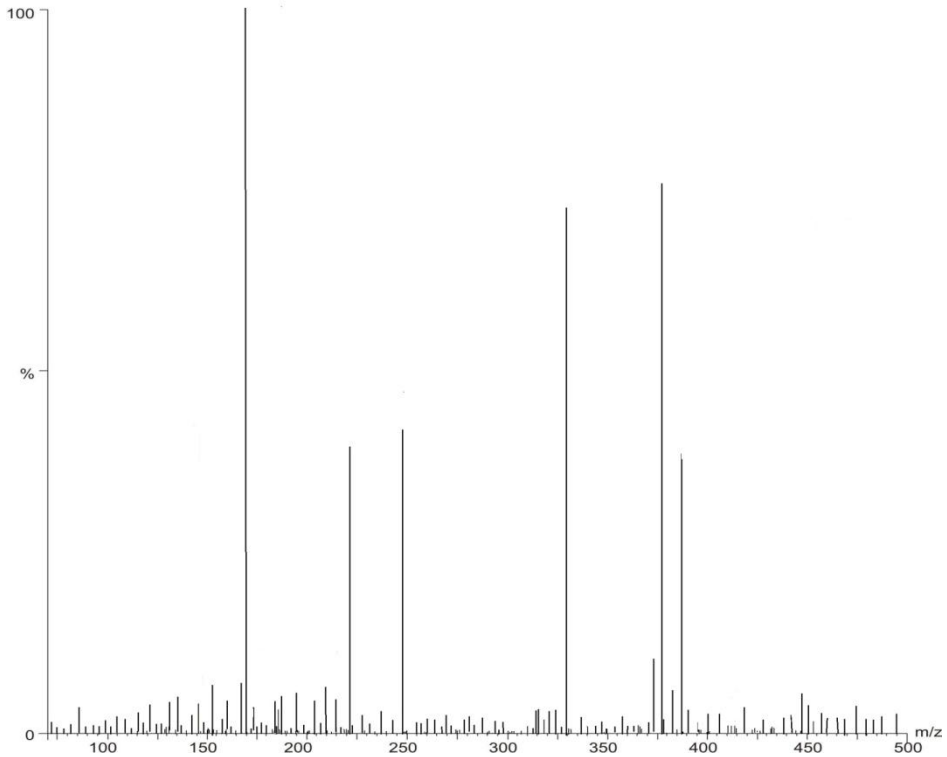

Fig.3b. TOF mass spectrum of the complex II

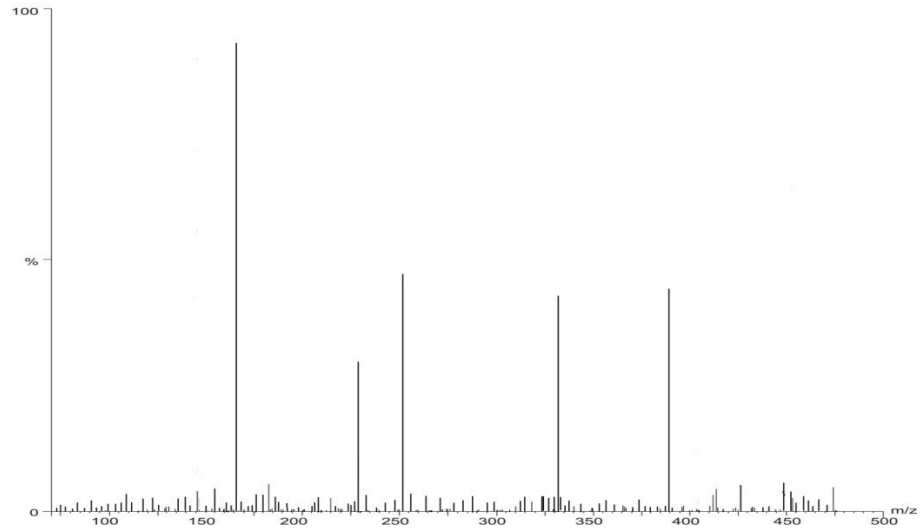

Fig.3c. TOF mass spectrum of the complex III

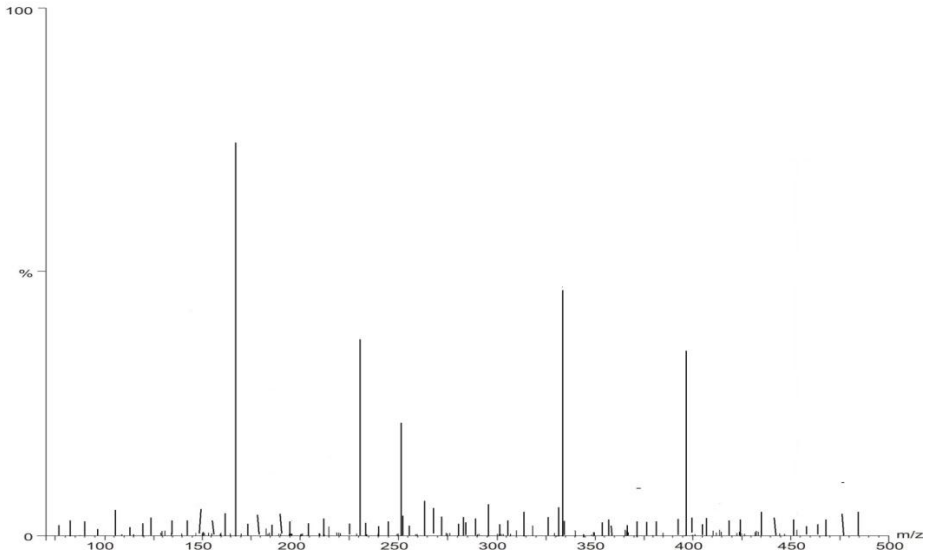

Fig.3d.TOF mass spectrum of the complex IV

3.2.Kinetics of thermal decomposition

Thermogravimetric (TG) and differential thermogravimetric analyses (DTA) were carried out for metal complexes in ambient conditions. The correlations between the different decomposition steps of the complexes with the corresponding weight losses are discussed in term of the proposed formula of the complexes. In the complexes, loss of ($C_2H_8O_2$) molecules takes place in the temperature range 473 – 573K followed by the decomposition of the organic moiety with the formation of metal oxide as

residue in the temperature range 660-890K[17]. This has been again confirmed by comparing the observed/estimated and the calculated mass of the pyrolysis product. On the basis of thermal decomposition, the thermodynamic activation parameters such as activation energy (E*), enthalpy of activation (ΔH*), entropy of activation (ΔS*), free energy change of decomposition (ΔG*) were evaluated(Table 2) by employing the Coats – Redfern relation [18]. The Coats and Redfern linearization plots for complexes (figure 4), confirms the first order kinetics for the decomposition process. According to the kinetic data obtained from the TG curves, all the complexes have negative entropy, which indicate that the complexes are formed spontaneously. The negative value of entropy indicates a more ordered activated state that may be possible through the chemisorptions of oxygen and other decomposition products. The negative values of the entropies of activation are compensated by the values of the enthalpies of activation, leading to almost the same values for the free energy of activation [17].

Table 2: Thermodynamic activation parameters of metal complexes

Complexes	Order(n)	Steps	E*(Jmol^{-1})	A($\times 10^5 s^{-1}$)	ΔS*(JK^{-1}mol^{-1})	ΔH*(J mol^{-1})	ΔG*(k J mol^{-1})
Complex I	1	I II	24.73 24.84	0.40 0.68	-256.53 -295.56	86.56 142.72	131.65 221.21
Complex II	1	I II	26.46 25.42	1.12 0.66	-144.36 -125.78	73.86 116.72	75.28 103.63
Complex III	1	I II	25.19 27.26	1.05 1.08	-248.62 -251.06	67.56 217.45	128.85 179.22
Complex IV	1	I II	26.40 29.56	2.51 1.99	-137.52 -135.65	86.56 142.72	72.69 113.14

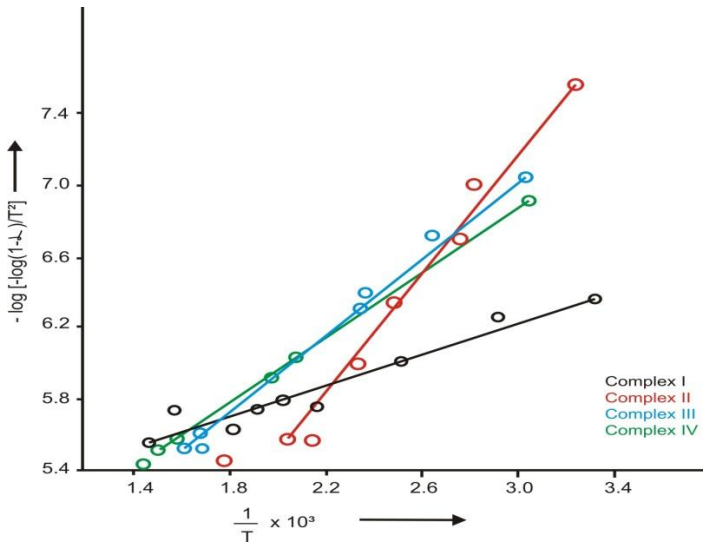

Figure 4: Kinetics of thermal decomposition of complexes

3.3Molecular Modeling Studies

Molecular mechanics attempts to reproduce molecular geometries, energies and other features by adjusting bond length, bond angles and torsion angles to equilibrium values that are dependent on the hybridization of an atom and its bonding scheme. In order to obtain estimates of structural details of these complexes, we have optimized the molecular structure of complexes. Energy minimization was repeated several times to find the global minimum. This supports square planar geometry of the metal complexes (Table 3: Bond angles and bond length of the complexes).

Table 3: Selected bond lengths(Å) and bond angle(^{0}) for complexes

Bonds		Complex I		Complex II		Complex III		Complex IV	
		bond angle	bond length	Bond angle	bond length	bond angle	bond length	bond angle	bond length
16-13-14	13-1	85.50	1.9237	90.47	1.8308	96.88	1.9353	99.66	2.0172
1-13-6	13-6	88.58	1.9109	94.25	1.8201	99.70	1.9088	98.01	1.9654
6-19-1	13-14	104.99	1.9191	97.95	1.8465	113.19	1.8732	111.53	2.0083
14-13-6	13-16	89.22	1.8768	77.89	1.8245	140.83	1.8968	113.07	2.0029
15-16-13	16-25	102.57	1.4275	104.89	1.3744	126.97	1.4837	122.86	1.4297
3-1-13	16-17	145.52	1.4424	107.48	1.3037	142.80	1.3879	126.20	1.3637
14-13-1	14-15	169.50	1.3364	170.69	1.3491	105.60	1.3055	111.53	1.2857
16-13-6	15-18	101.21	1.4764	166.02	1.4253	100.49	1.4781	113.07	1.4888
13-1-3	17-18	87.59	1.4346	130.52	1.4253	102.95	1.3974	118.68	1.4071
2-1-3	1-2	115.77	1.4289	118.78	1.4268	114.22	1.4654	114.97	1.4392
4-11-12	1-3	117.04	1.4004	116.01	1.3127	118.10	1.3076	117.28	1.3195
24-23-20	3-4	115.85	1.4304	115.18	1.4412	115.36	1.4603	114.88	1.4392
16-17-18	6-5	116.01	1. 3262	112.68	1.3209	123.01	1.3385	124.89	1.3108
13-14-15	5-4	40.89	1.5018	97.812	1.4257	121.96	1.4652	118.29	1.4271
25-16-17	4-11	111.39	1. 3766	129.73	1.3817	107.62	1.3784	112.80	1.3731
	11-12		1. 4094		1.4091		1.4077		1.4078
	20-23		1. 3801		1.3891		1.3868		1.3891
	23-24		1.4091		1.4082		1.4106		1.4112

The energy minimization value for square planar and without restricting the structure for the Co(II), Ni(II),Cu(II) and Zn(II) complexes are 7245kcal/mol with gradient 0.8459, 7239kcal/mol with gradient 0.8961, 7190kcal/mol with gradient 0.8671 and 7261kcal/mol with gradient 0.8823 respectively. The optimized molecular structures of the metal complexes are represented in Figure 5a-d. The energy minimization values for copper complex has minimum than nickel complex than cobalt complex than zinc complex which has maximum energy. It indicates copper complex has maximum stability than other metal complexes.

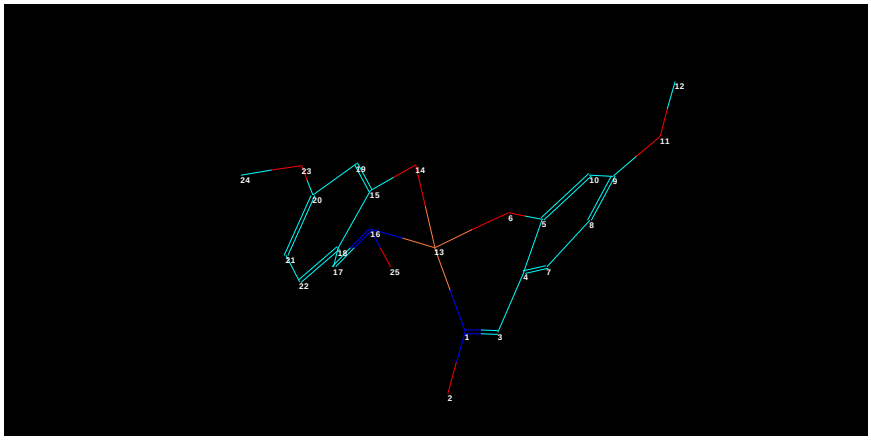

Fig. 5a: Optimized structure of complex I

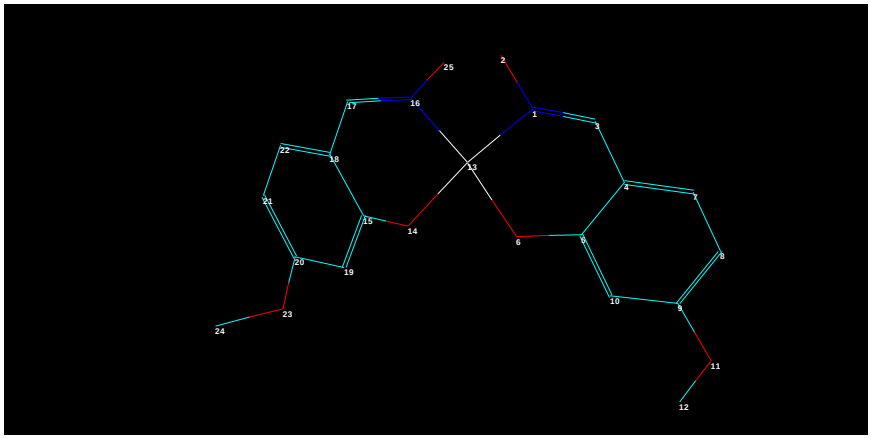

Fig. 5b: Optimized structure of complex II

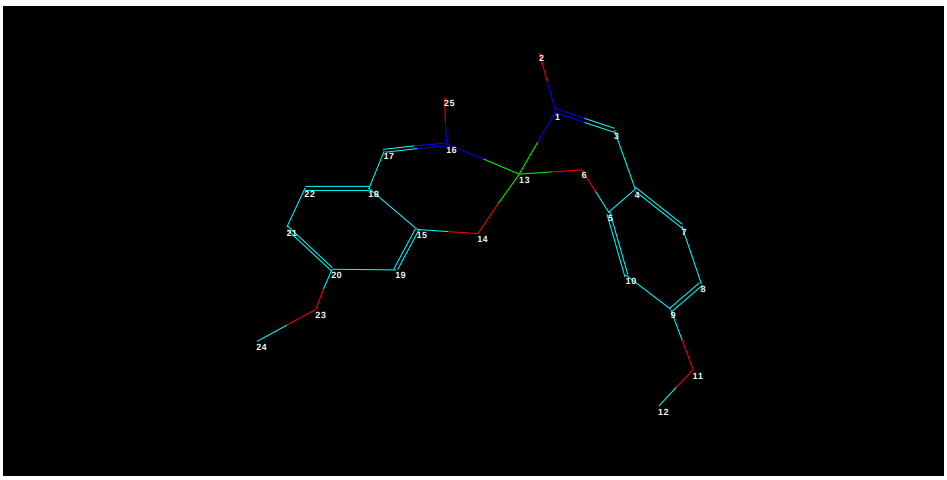

Fig. 5c: Optimized structure of complex III

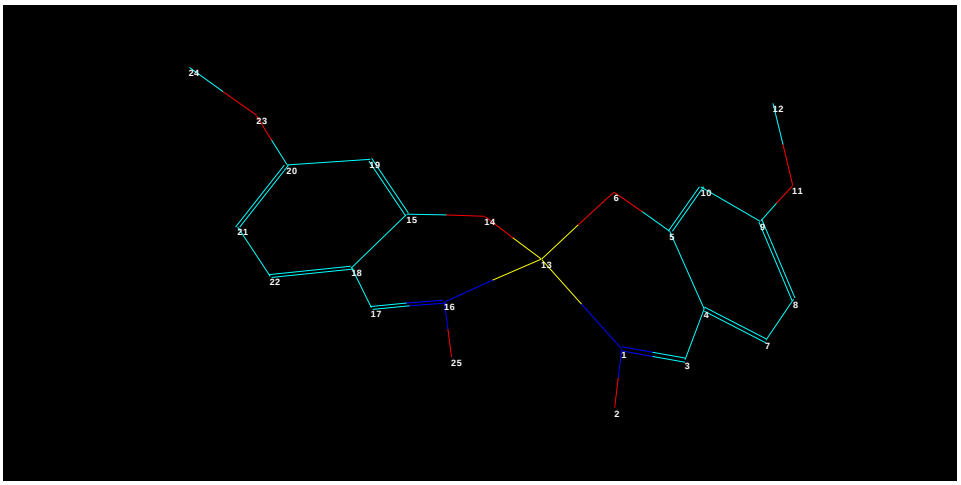

Fig. 5d: Optimized structure of complex IV

3.4 Biological studies

The free ligand(4-MEOSDOX) and its respective metal chelates were screened against*Streproproteus*, *Staph*, *Staphylococcus* and *E.coli*bacteria to assess their potential antimicrobial agents. The results are quite promising. The bacterial screening results (Fig. 6) reveal that the free ligand (4-MEOSDOX) and its metal complexes showed the maximum activity against *Streproproteus*bacteria. The complexes have maximum activity against*Streproproteus*bacteria followed by *Staphylococcus* bacteria except complex II has maximum activity against*Streproproteus*bacteria followed by*E.coli*bacteria. In general, the activity was the least against *Staph* bacteria. The antimicrobial data reveal that the complexes are more bioactive than the free ligand. The presence of nitrogen and oxygen donor groups in the synthesized compounds inhibited enzyme production because enzymes require free hydroxyl group for their activity appear to be especially susceptible to deactivation by the metal ion [17].

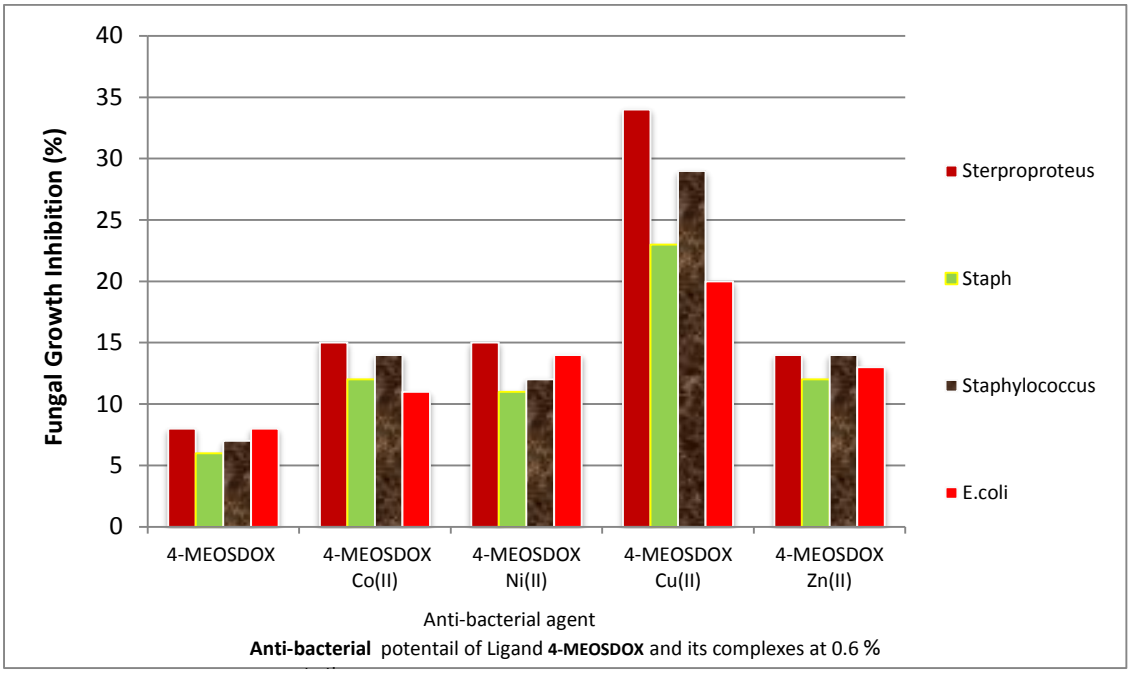

Fig.6a. Antibactrial potential of the ligand and its complexes at 0.6% concentration

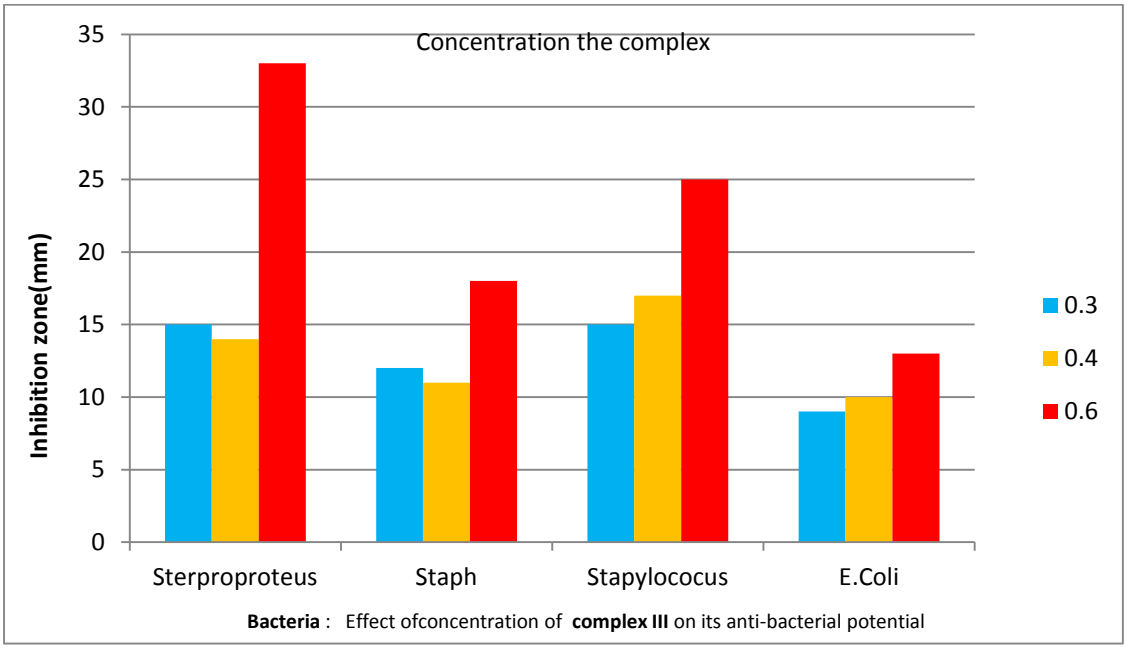

Fig.6b. Effect of concentration of the complex III on its anti-bacterial potential

Complexation reduces the polarity of the metal ion from partial sharing of its positive charge with the donor groups; π- electron delocalization in this chelating ring also increases the lipophilic nature of the metal atom, favoring permeation through the

lipid layer of the membrane. The enhanced activity of the metal complexes may be ascribed to the increased lipophilic nature of these complexes arising due to chelation [17]. It was also noted that the toxicity of the metal chelates increases on increasing the metal ion concentration. It is probably due to faster diffusion of the chelates as a whole through the cell membrane or due to the chelation theory. The bounded metal may block enzymatic activity of the cell or else it may catalyze toxic reactions among cellular constituents.

4. CONCLUSION

With the help of various physico-chemical techniques, geometries of the newly synthesized compounds have been proposed (Figure 7). The ligand acts as a bidentate ligand involved coordination with metal ions through the phenolic oxygen and the oxime nitrogen forming square planar complexes. Kinetics of thermal decomposition was computed from the thermal data using Coats and Redfern method, which confirm first order kinetics. The Cu(II) complex was found to be most active against the growth of bacteria.

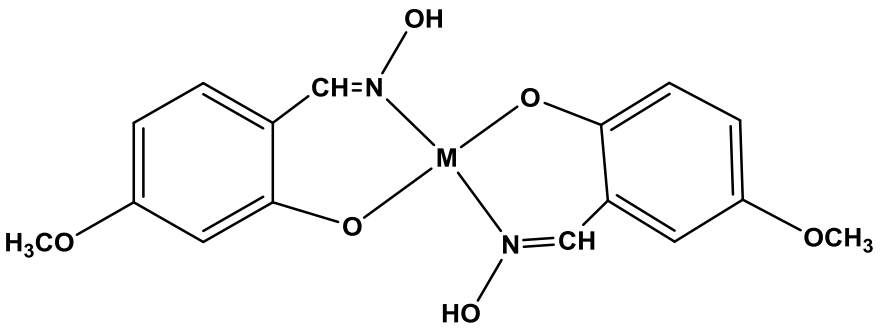

Fig 7: Structure of the proposed complexes

M= Co(II), Ni(II), Cu(II) and Zn(II)

ACKNOWLEDGEMENTS

The author(B K Singh) thankfully acknowledge to University Grants Commission(UGC), New Delhi, India for financial support.

REFERENCES

[1] (a) Durmus M., Dincer F., Ahsen V.,2008, Dyes and Pigments, 77,pp. 402-407.(b)Abele E., Lukevics E.,2000, Org Prep Proceed Int, 32, pp.235-264.(c) Chakravorty A.1974,CoordChem Rev., 13 pp.1-46.(d)Ramesh V.,Umasundari P., Das K. K.,1998,Spectrochim.Acta A 54,pp. 285–297.

[2] (a) Martinez J., Aiello I., Bellusci A.,Crispini A., Ghedini M., 2008,Inorganic ChimActa 361,pp. 2677-2682.(b)Gumus G., Ahsen V.,2000, Mol.

CrystLiqCryst. 348, pp.167-178.(c)Ohta K., Hasebe H., Moriya M., Fujimoto T.,Yamamoto I., 1991,Mol CrystLiqCryst 208,pp. 43-54.

[3] Jayaraju D.,Kondapi A. K.,2001, Current Science 81(7), pp**.** 787-792.

[4] Březina F., Tillmannová H., Šindelář Z.,1986,Chem. Papers , 40(6*)*,pp.727—733.

[5] Rajabi L., Courreges C., Montoya J., Aguilera R. J., Primm T. P.,2005,Lett. Appl. Microbiol. 40,pp. 212- 215.

[6] Hyperchem Release 7.51 Professional Version for Windows, Molecular Modeling System, Hyperchem Inc. Canada, 2005.

[7] Saxena C., Sharma D. K., Singh R. V.,1993, Phosphorous Sulfur Silicon 85(1-4),pp. 9-1.

[8] Omar M. M., Mohamed G. G.,2005,Spectrochim. Acta A, 61, pp.929-936.

[9] Georgieva I., Tredafilova N., Bauer G.,2006,Spectrochim. Acta A, 63,pp. 403-415.

[10] Nakamoto K., Infrared and Raman Spectra of Inorganic and Coordination Compounds, Wiley, New York, 1978.

[11] Silverstein R. M., Bassler O. G., Morrill T. C., Spectrophotometic Identification of Organic Compounds, Wiley, New York, 1974.

[12] Nakamoto K., McCarthy S.J., Spectroscopy & Structure of Metal Chelate Compounds,John Wiley & Sons, USA, 1968.

[13] Lever A.B. P., Inorganic Electronic Spectroscopy, Elsevier, Amsterdam, 1968.

[14] Figgis B. N., Introduction to Ligand Fields, 1st ed., 1966, p. 263.

[15] (a) Sanmartin J., Novio F., Garcia- Deibe A. M., Fondo M., Ocampo N., Bermejo M. R.,2006, Polyhedron, 25,pp. 1714-1722. (b) Singh B. K., Prakash A., Adhikari D.,2009,Spectrochim. Acta A, 74,pp. 657-664.(c) Singh B. K., Rajor H. K., Prakash A.,2012, Spectrochim. Acta A, 94, pp.143-151.(d) Beloso I., Castro J., Garcia-Vazquez J., Perez-Lourido A. P., Romero J., Sousa A.,2003, Polyhedron*,*22, pp.1099-1111.

[16] (a) Yoshida N., Ichikawa K., Shiro M. J.,2000,Chem. Soc.Parkin Trans. 2, pp.17-26. (b) Yoshida N., Oshio H., Ito T., 1999,J. Chem. Soc. Perkin Trans**.** 2, pp.975-984.(c) Singh B.K., Rajour H.K., Chauhan R., Goyal S.,2015, Chemical Sci. Trans. 4(3),pp. 806-818.

[17] (a) Singh B. K.,Sharma R. K., Garg B. S.,2006, J. Thermal Anal. Cal. 84,pp.593-600. (b) Prakash A., Singh B.K., Bhojak N, Adhikari D.,2010, SpectrochimActa A 76,pp. 356-362.

[18] Coats W, Redfern J.P.,1964, Nature,201 pp.68.

[19] (a) Ahamad T., Nishat N., Parveen S.,2008, J. Coord. Chem. 61, pp.1963-1972 (b) Singh B. K., Rajour H. K., Chandra J.,2016, J. Applied Chemical Sci. International, 6(1), pp. 45-57.(c) Singh B. K., Mishra P.,Prakash A.,Bhojak N.,2017, Arabian J Chem. 10,pp.S472-S483.